

Computational Exploration of the Photoprotective Potential of Gadusol

Raúl Losantos,^[a] M. Sandra Churio,^[b] and Diego Sampedro^{*[a]}

Gadusol shows one of the simplest structures among a series of natural UV-absorbing compounds that have been related to the photoprotective and antioxidant functions in aquatic organisms. CASPT2//CASSCF methodology was used to carry out a theoretical study on this basic structure in order to describe the underlying features responsible for the photoprotective capacity of the molecule. The influence of the enol–enolate equi-

librium on the photophysical properties was explored. The results confirm that both forms undergo a rapid deactivation, which very efficiently dissipates light energy as heat. This work highlights the potential of molecular-level studies to provide an understanding of natural photoprotective mechanisms and gives support to the future design of structurally related new synthetic sunscreens.

Introduction

Sunlight absorption by biological molecules plays a crucial role in life development and sustains the earth's energy cycle; as a counterpart, photoprotective mechanisms are necessary to minimize the potential damage of the UV portion of the solar spectrum that reaches organisms.^[1] The interest in natural UV photoprotection research has increased lately, given substantial losses in the stratospheric ozone layer and the consequent increase in UV radiation levels in the troposphere.^[2,3] One of the major strategies used by organisms to minimize UV-induced damage is screening by intra- or extracellular compounds that are able to block UV radiation.^[1,4,5] Mycosporine-like amino acids (MAAs) and gadusol (3,5,6-trihydroxy-5-hydroxymethyl-2-methoxycyclohex-2-en-1-one) belong to a series of natural UV-absorbing compounds that have been related to photoprotective and antioxidant functions in aquatic organisms.^[6–8] The photophysics and photochemistry of some of these secondary metabolites have been examined in aqueous solution.^[9–14] The main findings are: negligible fluorescence

yields, high photostability, and efficient dissipation of the absorbed radiation energy as heat. All these properties support the postulated sunscreensing role of the molecules. In fact, various reports indicate that MAAs are biosynthesized and accumulated in response to UV radiation, thus preventing damaging photons from reaching potential cellular targets and avoiding photosensitization processes by the favorable competition of thermal de-excitation pathways.^[5–7,15,16] However, the precise connection between these properties and the chemical structures of these compounds remains to be fully addressed. In that sense, it is interesting to examine some trends in the correlation of the available photophysicochemical data with the structural features of this family of natural molecules.

It has been reported that gadusol, mycosporine–glycine, mycosporine–taurine, and mycosporine–glutaminol–glucoside, all of which share a cyclohexenone core, are efficient antioxidants,^[6,17–19] whereas the imino-mycosporines shinorine and porphyra-334 are rather resistant to oxidation.^[20] The photodecomposition quantum yield of gadusol in aqueous solution is low, but is 100-fold greater than that of the conjugate anion gadusolate, the prevailing species under physiological pH.^[14]

It is known that cyclic α,β -unsaturated ketones produce relatively stabilized triplets if substituted at the β -carbon atom,^[21] however, no triplet state from gadusolate could be observed by direct laser photolysis. Moreover, interaction between gadusolate and some triplet sensitizers leads to reductive quenching of the latter.^[14] On the contrary, sensitization experiments have given evidence for only the energy transfer to yield the excited triplet states of the imino-MAAs shinorine, porphyra-334, and palythine.^[9,10,12]

In this context, calculation of the deactivation pathways can provide valuable information for rationalization of the experimental results and consequently potentiate the future design of new synthetic photoprotectors. Recently, a computational study using the CASPT2//CASSCF strategy was carried out on palythine, the simplest structure among imino-MAAs.^[22] The


[a] R. Losantos, Dr. D. Sampedro

Departamento de Química, Universidad de La Rioja
Centro de Investigación en Síntesis Química (CISQ)
Madre de Dios 51, 26006 Logroño (Spain)
E-mail: diego.sampedro@unirioja.es

[b] Dr. M. S. Churio

Departamento de Química
Facultad de Ciencias Exactas y Naturales
Universidad Nacional de Mar del Plata
Consejo Nacional de Investigaciones Científicas y Técnicas (CONICET)
Dean Funes 3350, B7602AYL, Mar del Plata (Argentina)

 Supporting information for this article is available on the WWW under <http://dx.doi.org/10.1002/open.201402125>: Cartesian coordinates for computed structures.

 © 2015 The Authors. Published by Wiley-VCH Verlag GmbH & Co. KGaA. This is an open access article under the terms of the Creative Commons Attribution-NonCommercial-NoDerivs License, which permits use and distribution in any medium, provided the original work is properly cited, the use is non-commercial and no modifications or adaptations are made.

fast relaxation on the excited-state energy surface via a conical intersection (CI) point is evident from this study. The main deformation of the structure corresponds to an out-of-plane movement of the imine moiety, while the adjacent carbon atoms approach each other and the alkene moiety remains almost planar. This result rules out the previously proposed deactivation pathway by simple C=N bond isomerization.^[12]

It is well established now that conical intersections mediate a variety of chemical events and have enormous relevance in biology, as they are responsible for the efficient internal conversion channels that recover DNA bases after sunlight activation in an ultrafast way.^[23,24] This suggests that DNA bases and MAA structures were naturally selected for their ability to dissipate energy.^[25]

Gadusol represents the basic molecular structure of the oxo-compounds mentioned above. At the same time, it allows exploration of the influence of the substituents in the conjugated system by simply shifting the enol–enolate equilibrium.^[26] A time-dependent density functional theory (TD-DFT) calculation of the transition energies for the enol form in water was carried out by Arbeloa et al.^[14] The results support the π – π^* assignment of the excited singlet state accordingly with the generalized solvatochromic shifts of the absorption spectra. However, no chemical calculation has been performed on gadusolate, the enolate form, which dominates the acid–base equilibrium under biological pH conditions. Herein we present the results of a theoretical study carried out with CASPT2//CASCF methodology in order to describe the underlying features responsible for the photoprotective role of gadusol. In turn, this information could be useful to understand the photoprotective mechanisms selected by natural evolution and for the design and synthesis of new and more efficient artificial sunscreens.

Results and Discussion

Initially we validated our model chemistry against the recorded UV spectra. The influence of the medium in the UV absorption of gadusol was recently reported.^[14] A bathochromic shift was observed as the polarity of the solvent increases. For instance, the maximum in the absorption band changes from 268 nm in water to 263 nm in acetonitrile; pH dependence was also observed in aqueous solution. For acidic solutions (pH 2.5) maximal absorption was found at 268 nm, whereas at higher pH values (pH \geq 7) an increase in band intensity was measured together with a bathochromic shift to 296 nm. These observations were explained on the basis of a displacement in the acid–base equilibrium between the neutral form (gadusol) present in acidic solutions and the enolate species (gadusolate) that dominates at pH 7, although the exact structure of the gadusolate re-

Table 1. Experimental and Franck–Condon vertical CASPT2 excitation energies, orbital transitions, and oscillator strengths (f) for gadusol and gadusolate in the gas phase.

Compound	Band [eV] (nm)	State	E_{CASPT2} [eV] (nm)	Transition	f	Relative f
gadusol	4.64 (268)	S_3	6.36 (195)	$^1(n,\pi^*)$	0.0002	5.7×10^{-4}
		S_2	5.23 (237)	$^1(\pi,\pi^*)$	0.35	1
		S_1	4.23 (293)	$^1(n,\pi^*)$	0.03	0.08
gadusolate	4.20 (296)	S_2	5.32 (233)	$^1(n,\pi^*)$	0.0004	4.1×10^{-4}
		S_1	5.00 (248)	$^1(\pi,\pi^*)$	0.97	1

mained unclear. Therefore, as an initial step we computed the UV spectrum of gadusol in the gas phase, and the results are summarized in Table 1.

It follows from these results that the computed CASPT2 UV spectrum for gadusol includes two $n \rightarrow \pi^*$ transitions to S_1 and S_3 with low oscillator strength values, as is usual for this type of transition. The relevant band corresponds to a $\pi \rightarrow \pi^*$ transition located at 237 nm with an oscillator strength of 0.35. Thus, the bright state in gadusol is S_2 , and this state will be mainly populated after radiation absorption. The experimental band maximum was reported to be 268 nm in water. Therefore, to determine the relevance of the solvent in our calculations, we computed the UV spectrum using the polarizable continuum model (PCM) with water and acetonitrile (Table 2). In both solvents, the state order was the same as that found in the gas phase, and the bright state was again S_2 with oscillator strength values of 0.25 (water) and 0.26 (acetonitrile), both similar to the value of 0.35 obtained in the gas phase. The computed maximum in water was located at 242 nm, whereas in acetonitrile the maximum appeared at 239 nm. Thus, the experimentally determined bathochromic shift is also qualitatively reproduced. The effect of the basis set was also explored by recomputing the absorption spectra in solvent with the ANO-L-VDZ basis set. In this case, the absorption in water was found at 245 nm, whereas in acetonitrile it appeared at 241 nm. As can be seen from the results in Tables 1 and 2, the CASPT2 values with 6-31G* in gas phase are qualitatively good enough to reproduce the experimental data.

Next, we explored the excited-state deactivation of gadusol after light absorption and population of the bright-state S_2 . The minimum energy path (MEP) computed for the relaxation along the S_2 potential energy surface (PES) is reported in Figure 1. Starting from the Franck–Condon region, very fast deactivation of S_2 is expected, as no minima or energy barriers were found before crossing between S_2 and S_1 at a CI point.

Table 2. Computed Franck–Condon vertical CASPT2 excitation energies for gadusol and gadusolate under various conditions.

Compound	E_{CASPT2} [eV] (nm)				
	Gas phase ^[a]	Water (PCM) ^[a]	CH ₃ CN (PCM) ^[a]	Water (PCM) ^[b]	CH ₃ CN (PCM) ^[b]
gadusol	5.23 (237)	5.12 (242)	5.04 (239)	4.91 (245)	5.14 (241)
gadusolate	4.85 (248)	4.71 (263)	4.77 (260)	4.54 (273)	4.63 (268)

[a] 6-31G* basis set. [b] ANO-L-VDZ basis set.

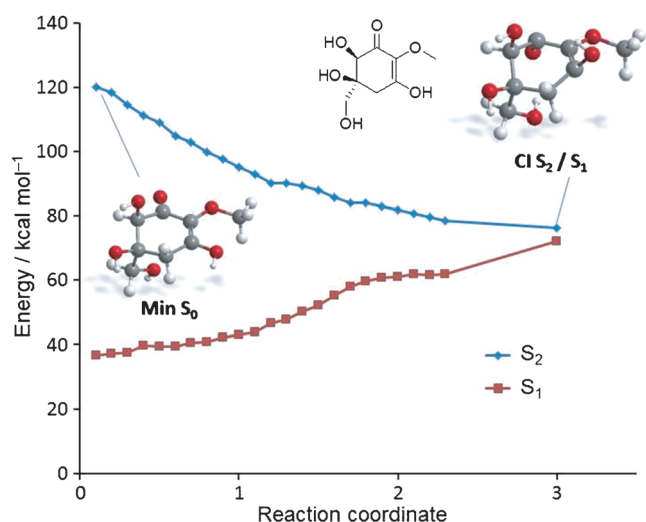


Figure 1. CASPT2 MEP for gadusol in S_2 . Energies are relative to ground-state minimum.

Once the $CI\ S_2/S_1$ point is reached, decay to S_1 can be easily achieved.

The main molecular distortion after relaxation in S_2 implies an out-of-plane movement of the oxygen atoms in the $C=O$ and OH moieties of the chromophore. Comparison between the structures of gadusol in the $Min\ S_0$ and $CI\ S_2/S_1$ structures shows that the molecule remains substantially planar in the ground state to minimize the energy through conjugation, whereas at the CI point the molecule is not planar due to partial breakage of the π system. The $C=O$ bond has an initial length in the ground state of 1.23 Å, while the length in the $CI\ S_2/S_1$ point is 1.34 Å. Also, the $C=C$ bond length changes from 1.35 to 1.49 Å. In addition, the $C=O$ and OH moieties at positions 1 and 3 of the chromophore move out of the plane of the molecule in the $CI\ S_2/S_1$ point (64° and -51° , respectively) in agreement with the $\pi \rightarrow \pi^*$ nature of the excited state.

Similarly, relaxation along the S_1 PES leads directly to a different CI point connecting with the ground state, as shown in Figure 2. Thus, ultrafast deactivation takes place in S_1 as well, as was predicted for S_2 . Accordingly, no significant fluorescence emission can be expected from gadusol. This result was experimentally verified previously.^[14]

Again, the main molecular distortions are related to breakage of the π system together with the out-of-plane movement of the oxygen atoms in the carbonyl and hydroxy groups that are part of the chromophore. This implies that the same molecular movements are involved in the deactivation in both S_2 and S_1 . In turn, this allows an ultrafast deactivation from the photon absorption to the ground-state recovery. The initial $C=O$ bond subsequently lengthens along the S_1 PES and at the $CI\ S_1/S_0$ point has a value of 1.58 Å.

Correspondingly, the initial $C=C$ bond reaches a value of 1.51 Å. The substituents at positions 1 and 3 are displaced from the plane of the molecule by 34° ($C=O$ moiety) and -65° (OH at position 3). The nuclear motion that lifts the degeneracy between the two states is represented by the gradient differ-

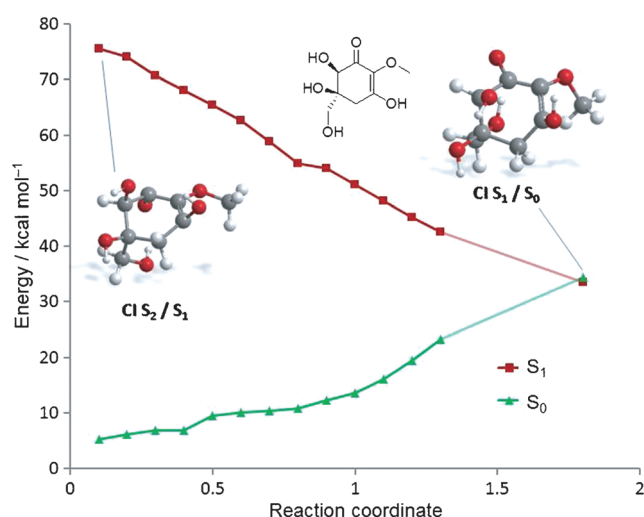


Figure 2. CASPT2 MEP for gadusol in S_1 . Energies are relative to ground-state minimum.

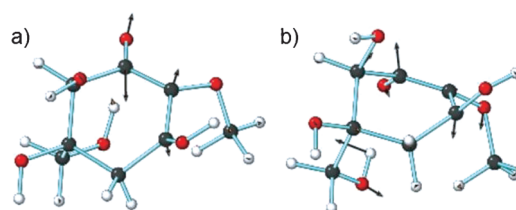


Figure 3. a) Derivative coupling (DC) and b) gradient difference (GD) vectors for gadusol $CI\ S_1/S_0$.

ence (GD) and derivative coupling (DC) vectors shown in Figure 3.

The nuclear motion pointed by the direction of the vectors suggests gadusol recovery once the ground state is reached. To check this, we optimized four different geometries in the ground state obtained from a slight distortion of the $CI\ S_1/S_0$ geometry in the directions marked by the DC and GD vectors. In all cases, the same geometry of the $Min\ S_0$ was found, probing the high photostability of gadusol. This is consistent with the low photodecomposition quantum yield experimentally determined in solution.^[14] This, together with the occurrence of two energetically accessible conical intersection points (CI), provides gadusol with excellent features as a photoprotective compound. These conical intersection points connect states S_2/S_1 and S_1/S_0 that can be reached by small geometrical changes, thus enabling the ultrafast decay from the Franck-Condon region to the ground state. The critical points along the gadusol PESs are summarized in Figure 4.

As stated above, the photophysical properties of gadusol were found to be pH dependent.^[14] To explain this behavior, we aimed at studying the enolate forms that could be present in neutral solutions. From the various alternatives that could be found in a neutral medium, we computed the two structures shown in Figure 5. These two structures correspond to deprotonation at two sites, both of which are considered to be capable of forming relatively stable anions.

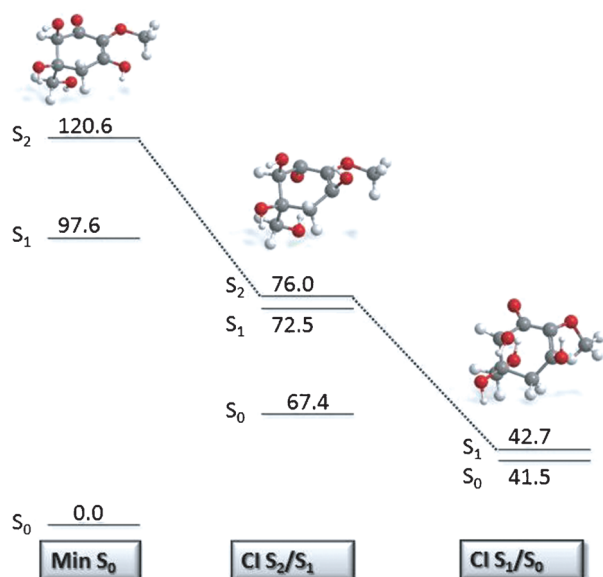


Figure 4. Critical points along the potential energy surface for gadusol. Energies are in kcal mol^{-1} , relative to the ground-state minimum.

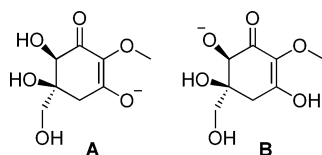


Figure 5. Computed structures for gadusolate.

Each of the structures in Figure 5 was computed in the gas phase and in water using the PCM method. In both cases structure **A** was found to be more stable than **B**. This is not surprising, as the enolate **A** can delocalize the negative charge along the π system, whereas the charge in enolate **B** is localized at the oxygen atom. This causes structure **A** to have similar C–O (1.23 Å in both cases) and C–C (1.42 and 1.40 Å) distances. However, structure **B** features clearly distinct C–O (1.21 vs. 1.34 Å) and C–C (1.47 and 1.33 Å) bond lengths. In addition, the relative energies of these two species show that no mixture of compounds should be present in neutral solutions of gadusol, as the energy difference is, in any case, very high. Results from CAS(16,10)/6-31G* with PCM indicate that enolate **A** is $42.5 \text{ kcal mol}^{-1}$ more stable than **B**. Thus, in the study of gadusol in aqueous solution, we performed our calculations exclusively on enolate **A**. The gas-phase absorption spectrum was computed, and the results are summarized in Table 1. A strong absorption ($f=0.97$) centered at 248 nm and characterized by a $^1(\pi,\pi^*)$ transition was found for S_1 , while S_2 shows $^1(n,\pi^*)$ character with a very small oscillator strength. This is consistent with the experimental band maximum found for gadusol at pH 7.^[14] The inclusion of water in the calculations by using PCM does not affect the qualitative picture, and the bright state is also S_1 , with an oscillator strength value of 0.91 and a band centered at 263 nm. The use of the ANO-L-VDZ basis set yields a band at 273 nm. Comparison between gadusol and gadusolate absorption spectra denotes some differ-

ences. First, in the gas phase the band maximum for gadusolate appears at 248 nm, whereas for gadusol the maximum is located at 237 nm. Also, gadusolate has a much more intense absorption ($f=0.97$ vs. 0.38). Thus, gadusolate, the main species present in neutral aqueous solutions under pseudophysiological conditions, shows both a higher and red-shifted absorption relative to gadusol. These two characteristics suggest an increased efficiency of gadusolate in terms of the photoprotective role in a natural environment. Also, as S_1 is the bright state, gadusolate could have a far simpler deactivation pathway to dissipate the light energy, thus implying an improved performance. So far this observation is in agreement with the experimentally observed lower photodecomposition quantum yield for gadusolate than for gadusol.^[14] To determine the photoprotective capacity of gadusolate, we computed the reaction pathway starting from the Franck–Condon region in S_1 . The results are shown in Figure 6.

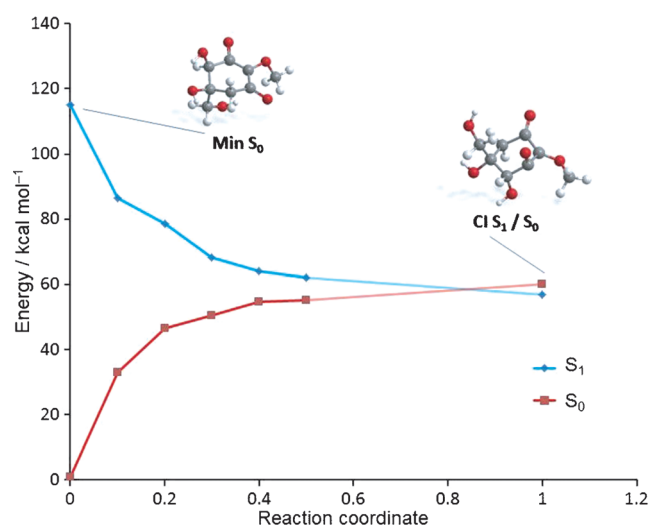


Figure 6. CASPT2 MEP for gadusolate in S_1 . Energies are relative to ground-state minimum.

After light absorption, relaxation of gadusolate along the S_1 PES leads directly to a CI point connecting with the ground state. Interestingly, the path connecting the Franck–Condon region with the CI point implies an ultrafast deactivation of the excited gadusolate, as no energy barrier is located along the reaction path. The main geometry deformation is the out-of-plane motion of the negatively charged oxygen atom of the chromophore (-71°) together with the C=C bond elongation (from 1.40 Å in **Min S₀** to 1.45 Å at the CI point). In contrast, the C=O bond length remains unaltered (1.23 Å in both geometries) with a small out-of-plane displacement of 45° . This deformation is similar to the geometry found for the CI points in related compounds, such as gadusol or palythine.^[22]

The branching plane for this CI is characterized by the DC and GD vectors shown in Figure 7. As expected, the nuclear motion that lifts the degeneracy between the states corresponds to the arrangement of the nuclei that make part of the chromophore, keeping the rest of the molecule almost unal-

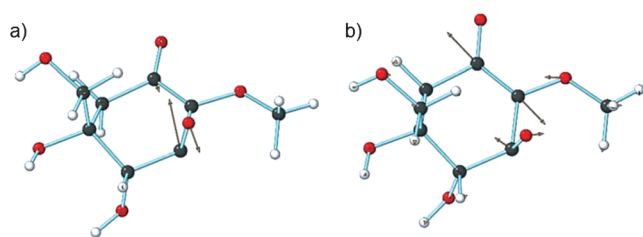


Figure 7. a) Derivative coupling (DC) and b) gradient difference (GD) vectors for gadusolate CI S_1/S_0 .

tered. Thus, it seems that both the excitation and geometry deformation are mainly located in just a part of the molecule. From a photophysical point of view, the photostability of gadusol is mainly due to the substituted cyclohexenone moiety, and the rest of the molecule is not relevant for the relaxation pathways of the excited state.

Deformation of the CI point geometry in the directions indicated by the two vectors leads to direct recovery of the starting material. Thus, no side-products are expected after irradiation of gadusolate which may account for the photodecomposition of this compound. This property is relevant for the photoprotective capacities of this type of metabolite. The critical points along the gadusolate PESs are summarized in Figure 8.

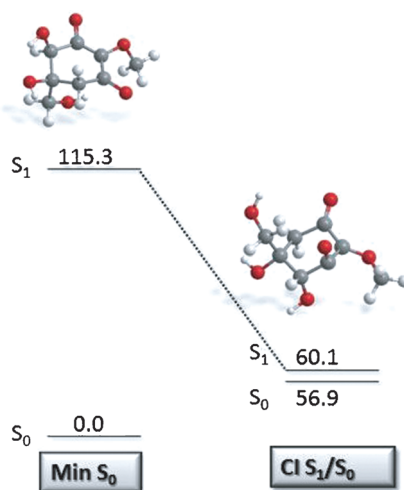


Figure 8. Critical points along the potential energy surface for gadusolate. Energies are in kcal mol⁻¹, relative to the ground-state minimum.

Conclusions

As shown by the theoretical calculations, although the deprotonated form of gadusol is responsible for the main absorption at pH 7 and thus it is the relevant species under physiological conditions, both gadusol and gadusolate share some photochemical features that confer these compounds a remarkable UV-protective capacity. Both forms allow rapid deactivation, which very efficiently dissipates light energy as heat. This is particularly significant in gadusolate, given the stronger absorption band. Also, the absence of any intermediates along the reaction paths is in agreement with the lack of fluorescence observed for these compounds. This fact, together with

the recovery of the starting material after irradiation supported by the low decomposition quantum yields, imparts high photostability to these molecules, which in turn allows for efficient energy wastage through subsequent photocycles. The photoprotective mechanism of gadusol and gadusolate is very similar to that previously described for MAAs.^[9,10,12,14,22] This also suggests the relation between gadusol and MAAs in terms of metabolic routes or even as different steps in the evolution of natural photoprotective compounds. The structural and mechanistic information provided by the molecular-level study of the photoprotective capacities of these and related compounds could encourage the design of new and more efficient products with interesting properties as sunscreens for commercial applications.

Experimental Section

Computational details: The most stable ground-state conformation was selected as the starting structure for the complete photochemical study, performed at *Multi-State Complete Active Space Perturbation to Second Order with a Complete Active Space Self-Consistent Field* reference wavefunction (i.e., MS-CASPT2//SA-CASSCF methodology).^[27,28] This methodology has already shown success in describing the photochemistry of various molecular systems.^[29,30] For this study, the *State Averaged-Complete Active Space Self-Consistent Field* (SA-CASSCF) method^[27] was used for calculation of the electronic transitions and the computed minimum energy paths (MEPs), including four states (S_0 , S_1 , S_2 , and S_3) with the same weight in the averaged wavefunction. The active space chosen comprises all the π and π^* orbitals together with the n orbitals of the oxygen atoms that influence the chromophore (16 electrons in 10 orbitals). Both CASSCF and CASPT2 calculations were performed with the standard 6-31G* basis set. The UV spectra were also computed by using the ANO-L-VDZ basis set. MEPs were computed at the CASSCF level with the methodology present in MOLCAS-6.4.^[31] MEPs representing steepest descendent minimum-energy reaction paths were built through a series of geometry optimizations, each requiring minimization of the potential energy on a hyperspherical cross-section of the potential energy surface (PES) centered on a given reference geometry and characterized by a predefined radius. The paths were computed by taking a value of 0.1 amu for the steps. Starting from the Franck-Condon (FC) structure, the path was followed to a conical intersection point. Once each new structure was obtained, this was taken as the new hypersphere center, and the procedure was iterated until the bottom of the energy surface was reached. Bulk solvent effects on the UV spectra were included by using the polarizable continuum model (PCM)^[32] as implemented in MOLCAS-6.4. The molecule is considered as included in a cavity surrounded by an infinite medium with the dielectric constant corresponding to the specific solvent. The standard values of 78.4 for water and 38.8 for acetonitrile were considered in these calculations. The UV spectra were computed under non-equilibrium conditions, that is, only solvent electronic polarization is in equilibrium with excited-state electron density. Thus, only fast solvent degrees of freedom are considered. This kind of calculation is more adequate to compute vertical excitation energies, as those needed for the UV spectra. Calculations of the gradient difference (GD) and derivative coupling (DC) vectors were performed with the Gaussian 03 software package,^[33] and MOLCAS 6.4 was used for calculation of the MEPs and CASPT2 single-point energy corrections.

Acknowledgements

This research was supported by the Spanish MICINN (CTQ2011-24800). M.S.C. thanks CONICET (PIP-0211), UNMDP (15-E611), and Programa de Fortalecimiento de Redes Interuniversitarias, PPUA-SPU Ministerio de Educación de la Nación (Argentina) for financial support.

Keywords: ab initio calculations · absorption · conical intersections · energy conversion · photochemistry

- [1] C. S. Cockell, J. Knowland, *Biol. Rev.* **1999**, *74*, 311–345.
- [2] United Nations Environment Programme, Environmental Effects Assessment Panel, A. L. Andradý, P. J. Aucamp, A. T. A. F. C. L. Ballaré, L. O. Björn, J. F. Bornman, M. Caldwell, A. P. Cullen, D. J. Erickson, F. R. de Gruijl, D. P. Häder, W. He, M. Ilyas, J. Longstreth, R. Lucas, R. L. McKenzie, S. Madronich, M. Norval, N. D. Paul, H. H. Redhwi, S. Robinson, M. Shao, K. R. Solomon, B. Sulzberger, Y. Takizawa, X. Tang, A. Torikai, J. C. van der Leun, C. E. Williamson, S. R. Wilson, R. C. Worrest, R. G. Zepp, *Photochem. Photobiol. Sci.* **2012**, *11*, 13–27.
- [3] D. P. Häder, E. W. Helbling, C. E. Williamson, R. C. Worrest, *Photochem. Photobiol. Sci.* **2011**, *10*, 242–260.
- [4] S. Roy in *The Effects of UV Radiation in the Marine Environment* (Eds.: S. de Mora, S. Demers, M. Vernet), Cambridge University Press, Cambridge, **2000**, pp. 177–205.
- [5] Q. Gao, F. Garcia-Pichel, *Nat. Rev. Microbiol.* **2011**, *9*, 791–802.
- [6] J. M. Shick, W. C. Dunlap, *Annu. Rev. Physiol.* **2002**, *64*, 223–262.
- [7] W. M. Bandaranayake, *Nat. Prod. Rep.* **1998**, *15*, 159–172.
- [8] J. I. Carreto, M. O. Carignan, *Mar. Drugs* **2011**, *9*, 387–446.
- [9] F. R. Conde, M. S. Churio, C. M. Previtali, *J. Photochem. Photobiol. B* **2000**, *56*, 139–144.
- [10] F. R. Conde, M. S. Churio, C. M. Previtali, *Photochem. Photobiol. Sci.* **2004**, *3*, 960–967.
- [11] K. Whitehead, J. I. Hedges, *J. Photochem. Photobiol. B* **2005**, *80*, 115–121.
- [12] F. R. Conde, M. S. Churio, C. M. Previtali, *Photochem. Photobiol. Sci.* **2007**, *6*, 669–674.
- [13] M. Moliné, E. M. Arbeloa, M. R. Flores, D. Libkind, M. E. Farias, S. G. Bertolotti, M. S. Churio, M. R. van Broock, *Radiat. Res.* **2011**, *175*, 44–50.
- [14] E. M. Arbeloa, S. G. Bertolotti, M. S. Churio, *Photochem. Photobiol. Sci.* **2011**, *10*, 133–142.
- [15] P. J. Neale, A. T. Banaszak, C. R. Jarriel, *J. Phycol.* **1998**, *34*, 928–938.
- [16] D. Libkind, P. A. Perez, R. Sommaruga, M. C. Diéguez, M. Ferraro, S. Brizio, H. Zagarese, M. R. Rosa Giraud, *Photochem. Photobiol. Sci.* **2004**, *3*, 281–286.
- [17] E. M. Arbeloa, M. J. Uez, S. G. Bertolotti, M. S. Churio, *Food Chem.* **2010**, *119*, 586–591.
- [18] W. C. Dunlap, Y. Yamamoto, *Comp. Biochem. Physiol.* **1995**, *112B*, 105–114.
- [19] H.-J. Suh, H.-W. Lee, J. Jung, *Photochem. Photobiol.* **2003**, *78*, 109–113.
- [20] F. de La Coba, J. Aguilera, F. L. Figueroa, M. V. de Gálvez, E. Herrera, *J. Appl. Phycol.* **2009**, *21*, 161–169.
- [21] D. I. Schuster, D. A. Dunn, G. E. Heibel, P. B. Brown, J. M. Rao, J. Woning, R. Bonneau, *J. Am. Chem. Soc.* **1991**, *113*, 6245–6255.
- [22] D. Sampedro, *Phys. Chem. Chem. Phys.* **2011**, *13*, 5584–5586.
- [23] L. González, D. Escudero, L. Serrano-Andrés, *ChemPhysChem* **2012**, *13*, 28–51.
- [24] a) C. E. Crespo-Hernández, B. Cohen, P. M. Hare, B. Kohler, *Chem. Rev.* **2004**, *104*, 1977–2019; b) S. Perun, A. L. Sobolewski, W. Domcke, *J. Phys. Chem. A* **2006**, *110*, 13238–13244.
- [25] L. Serrano-Andrés, M. Merchán, *J. Photochem. Photobiol. C* **2009**, *10*, 21–32.
- [26] a) P. T. Grant, P. A. Plack, R. H. Thomson, *Tetrahedron Lett.* **1980**, *21*, 4043–4044; b) P. A. Plack, N. W. Fraser, P. T. Grant, C. Middleton, A. I. Mitchell, R. H. Thomson, *Biochem. J.* **1981**, *199*, 741–747.
- [27] B. O. Roos, P. R. Taylor, P. E. M. Siegbahn, *Chem. Phys.* **1980**, *48*, 157–173.
- [28] K. Andersson, P.-Å. Malmqvist, B. O. Roos, *J. Chem. Phys.* **1992**, *96*, 1218–1226.
- [29] *Computational Photochemistry* (Ed.: M. Olivucci), Elsevier, Amsterdam, **2005**.
- [30] D. Sampedro in *Photochemistry: UV/Vis Spectroscopy, Photochemical Reactions and Photosynthesis* (Eds.: K. J. Maes, J. M. Willems), Nova Science Publishers, New York, **2011**.
- [31] G. Karlström, R. Lindh, P.-Å. Malmqvist, B. O. Roos, U. Ryde, V. Veryazov, P.-O. Widmark, M. Cossi, B. Schimmelpfennig, P. Neogrady, L. Seijo, *Comput. Mater. Sci.* **2003**, *28*, 222–239.
- [32] J. Tomasi, B. Mennucci, R. Cammi, *Chem. Rev.* **2005**, *105*, 2999–3094.
- [33] M. J. Frisch, G. W. Trucks, H. B. Schlegel, G. E. Scuseria, M. A. Robb, J. R. Cheeseman, J. A. Montgomery, Jr., T. Vreven, K. N. Kudin, J. C. Burant, J. M. Millam, S. S. Iyengar, J. Tomasi, V. Barone, B. Mennucci, M. Cossi, G. Scalmani, N. Rega, G. A. Petersson, H. Nakatsuji, M. Hada, M. Ehara, K. Toyota, R. Fukuda, J. Hasegawa, M. Ishida, T. Nakajima, Y. Honda, O. Kitao, H. Nakai, M. Klene, X. Li, J. E. Knox, H. P. Hratchian, J. B. Cross, C. Adamo, J. Jaramillo, R. Gomperts, R. E. Stratmann, O. Yazyev, A. J. Austin, R. Cammi, C. Pomelli, J. W. Ochterski, P. Y. Ayala, K. Morokuma, G. A. Voth, P. Salvador, J. J. Dannenberg, V. G. Zakrzewski, S. Dapprich, A. D. Daniels, M. C. Strain, O. Farkas, D. K. Malick, A. D. Rabuck, K. Raghavachari, J. B. Foresman, J. V. Ortiz, Q. Cui, A. G. Baboul, S. Clifford, J. Cioslowski, B. B. Stefanov, G. Liu, A. Liashenko, P. Piskorz, I. Komaromi, R. L. Martin, D. J. Fox, T. Keith, M. A. Al-Laham, C. Y. Peng, A. Nanayakkara, M. Challacombe, P. M. W. Gill, B. Johnson, W. Chen, M. W. Wong, C. Gonzalez, and J. A. Pople, *Gaussian 03, Revision C.02*, Gaussian, Inc., Wallingford CT, **2004**.

Received: November 21, 2014

Published online on March 9, 2015